

Concept Paper

Not peer-reviewed version

A Structural Causal Model for Robot-Assisted Upper-Limb Neurorehabilitation

[Sivakumar Balasubramanian](#) *

Posted Date: 28 February 2026

doi: 10.20944/preprints202602.1928.v1

Keywords: robot-assisted therapy; stroke; upper-limb rehabilitation; structural causal model; directed acyclic graph; precision neurorehabilitation; mechanistic modeling



Preprints.org is a free multidisciplinary platform providing preprint service that is dedicated to making early versions of research outputs permanently available and citable. Preprints posted at Preprints.org appear in Web of Science, Crossref, Google Scholar, Scilit, Europe PMC.

Copyright: This open access article is published under a [Creative Commons CC BY 4.0 license](#), which permit the free download, distribution, and reuse, provided that the author and preprint are cited in any reuse.

Disclaimer/Publisher's Note: The statements, opinions, and data contained in all publications are solely those of the individual author(s) and contributor(s) and not of MDPI and/or the editor(s). MDPI and/or the editor(s) disclaim responsibility for any injury to people or property resulting from any ideas, methods, instructions, or products referred to in the content.

Concept Paper

A Structural Causal Model for Robot-Assisted Upper-Limb Neurorehabilitation

Sivakumar Balasubramanian

Department of Bioengineering, Christian Medical College Vellore, Vellore, Tamil Nadu, India; siva82kb@cmcvellore.ac.in

Abstract

Upper-limb robot-assisted neurorehabilitation in stroke yields modest improvement in impairments, with substantial variability across patients. In response, there is increasing interest in precision neurorehabilitation through mechanistically driven, tailored robot-assisted therapy for individual patients. Such approaches require models that support interventional reasoning about therapy parameters (e.g., “what if we increase robotic assistance or dose for this patient?”), rather than providing purely associational findings such as biomarkers correlated with recovery. Leveraging recent developments in causal inference, this paper presents a structural causal model of robot-assisted therapy for the upper limb in the form of a directed acyclic graph. The graph encodes key constructs identified in the robot-assisted neurorehabilitation literature as nodes and represents their known or hypothesized causal influences as directed edges, reflecting current domain knowledge. We describe the components of the causal graph in detail and show how it can account for several observed phenomena in robot-assisted therapy, while also yielding testable predictions in the form of interventional effects. We then highlight important limitations of the proposed causal model, before presenting a conceptual example of how a fully specified causal graph could help answer questions about attainable outcomes and optimal therapy parameters for individual patients. The proposed concrete causal graph must be empirically investigated to test its validity and refine its causal structure through observational and experimental studies. We anticipate that this proposed causal graph will serve a catalytic role in advancing our mechanistic understanding of robot-assisted therapy, which may hold the key toward improving individual patient outcomes with robot-assisted therapy.

Keywords: robot-assisted therapy; stroke; upper-limb rehabilitation; structural causal model; directed acyclic graph; precision neurorehabilitation; mechanistic modeling

1. Introduction

“Problems are inevitable. Problems are soluble.”

— David Deutsch, *The Beginning of Infinity*

The last three decades have seen a tremendous activity in the development and clinical evaluation of a wide range of robotic devices [1] for upper-limb (UL)¹ therapy following stroke. Although most current UL rehabilitation robots are complex, expensive, and mostly restricted to the clinic, there is an increasing trend towards simpler, portable, and affordable devices designed to work across the continuum of care [2–6]. These devices present new opportunities for increasing therapy dose beyond what is possible with conventional therapy [3].

Existing clinical evidence for UL robot-assisted therapy (RAT) in stroke indicates that robots can safely provide high intensity therapy; they can support hundreds of movements in a session [7]. A recent meta-analysis by de Iaco et al., which included 90 randomized controlled trials (≈ 2500 subjects), found that UL RAT shows a small improvement of ≈ 2 points on the UL Fugl-Meyer Assessment

¹ Shoulder, elbow, wrist and/or hand.

(FMA) scale [8]. However, these small improvements in motor impairments do not generalize to UL capacity [8], i.e., the ability to lift/carry objects, fine hand function, etc. [8] also observed substantial response heterogeneity in the UL FMA scores in their meta-analysis (supplementary figure with the forest plot); response heterogeneity is a common problem in medical treatments [9,10]. The recent call for precision neurorehabilitation [11–14] is an effort to minimize this response heterogeneity through tailored interventions and maximize individual treatment responses. [8] concluded their meta-analysis with a recommendation for mechanistically-driven development of future RAT. A mechanistic model of RAT can provide the scaffold to build precision neurorehabilitation approaches. Such a model has been called by different terms in the current literature, such as computational neurorehabilitation model [14], digital twin [13], or a causal model [12].

Previous studies have identified biomarkers of spontaneous or therapy-driven post-stroke recovery [11,15–19]. The PREP2 algorithm uses the shoulder-abduction-finger-extension (SAFE) score along with motor evoked potential (MEP) measurements or brain imaging data, early after stroke, to predict the amount of UL function at 6 months post-stroke [20,21]. The presence or absence of MEP has been found to be a good predictor of the amount of UL impairments as measured by the FMA [22]. The extent of injury to the motor tracts measured through brain imaging predicted the sensorimotor gains following robot-assisted hand therapy [17]. Another study found that the somatosensory integrity of the paretic hand predicted therapy-driven gains in robot-assisted finger therapy [16]. A recent three-arm randomized controlled trial found that proprioceptive status of the fingers can predict responsiveness to robotic and non-robotic therapy [19]. These are examples of associative models that identify specific factors or biomarkers correlated with recovery, which can be used for patient stratification, as was suggested by [19]. Although, these studies are important steps towards a deeper understanding of RAT and developing precision neurorehabilitation strategies, further work is needed to build a comprehensive mechanistic model of RAT that can be exploited for optimal therapy prescription.

Frameworks for such models exist in the current literature. [14] proposed the idea of *computational neurorehabilitation* models that are detailed, mechanistic dynamical models typically in the form of differential equations modeling the neural plasticity and sensorimotor recovery processes employing physiologically meaningful latent and observable states. [13] proposed the idea of *digital twins* for neurorehabilitation, which are virtual replicas of the patient and their recovery process that can be used to simulate and optimize therapy. They advocate the use of *collaborative AI* for this purpose. [12] proposed the use of *causal models* to understand the mechanisms underlying recovery and to guide therapy decisions. These three frameworks share the common goal of capturing the causal, mechanistic process underlying sensorimotor recovery, albeit through different approaches and varying levels of detail. They also differ from the associational models discussed before in that they enable interventional reasoning, i.e., what will happen if we administer an intervention or change a therapy parameter.

Taking heed of the growing call for theory-driven approaches in rehabilitation [8,12,14,23,24], and drawing on causal inference methods [25–27], this paper proposes a structural causal model (SCM) for RAT for UL stroke neurorehabilitation. The model synthesizes current evidence for RAT-driven sensorimotor recovery, explicitly stating its mechanistic assumptions and hypotheses. We first present a general computational neurorehabilitation-type model of sensorimotor recovery, from which a simplified RAT-specific SCM is derived. We then provide a detailed description of the proposed model, which includes the definition of the SCM's components and their hypothesized causal links. Following this, we discuss the implications of this proposed model, and its current limitations. Finally, we conclude with a demonstration of the use of such a model for precision neurorehabilitation for individual patients.

2. A General Dynamic Model of Sensorimotor Recovery in Neurorehabilitation

“Imagine how much harder physics would be if electrons had feelings.”

— Richard Feynman

Motor recovery is a complex, continuous-time dynamic process affected by various subject-specific, environmental, and therapy-related factors. The knowledge of the underlying laws governing this process would empower clinicians to maximize recovery for individual patients through personalized therapy. A computational neurorehabilitation [14] model can capture this process through a mechanistic state-space vector differential equation, given as follows,

$$\begin{aligned}\dot{\mathbf{x}}(t) &= \mathbf{f}(\mathbf{x}(t), \mathbf{u}(t); \mathbf{p}) \\ \mathbf{y}(t) &= \mathbf{g}(\mathbf{x}(t); \mathbf{p}) + \epsilon\end{aligned}\quad (1)$$

where, \mathbf{x} is the state vector of interacting factors relevant to the recovery process, spanning the physiological, biomechanical, and psychological domains. Some examples of these factors include, the state of the penumbra (relevant in the acute and subacute stage), neuronal excitability, resting state connectivity, sensory acuity, motor coordination, and intrinsic motivation. While the state vector captures time-varying factors involved in the recovery process, the parameter vector \mathbf{p} constitutes subject-specific (quasi-) stable traits, that moderate the interaction between the state variables. This includes factors such as age, education, cognitive reserve, lesion characteristics, residual corticospinal tract integrity, personality, caregiver/family support, and socioeconomic context. The vector \mathbf{u} is the list of intervention variables under the clinician's control. These include, prescribed dose and intensity, task complexity, therapy modality, and feedback modality and schedule. The function \mathbf{f} captures how state variables (\mathbf{x}), the intervention variables (\mathbf{u}), and the parameter vector (\mathbf{p}) interact and influence the temporal evolution of the state ($\dot{\mathbf{x}}$). The state vector is often not directly measurable, but influences the measurable variables represented by the measurement vector \mathbf{y} . The measurement vector \mathbf{y} could include standard clinical assessments (e.g., Fugl-Meyer assessment, action research arm test), quantitative sensorimotor assessments (e.g., range of motion, muscle strength, movement smoothness), UL functioning [28], patient reported outcomes (e.g., motor activity log), neurophysiological measures (e.g., EMG, motor evoked potentials, and resting state EEG). The relationship between the measurement vector \mathbf{y} and the state vector \mathbf{x} is captured by the function \mathbf{g} . The vector ϵ represents output measurement noise, along with unmodeled dynamics affecting state evolution.

Using the dynamic model in Eq. 1, choosing an optimal therapy program or policy to efficiently maximize recovery can be posed as the following constrained optimization problem,

$$\begin{aligned}\mathbf{u}^*(t) &= \arg \max_{\mathbf{u}(t)} J(\mathbf{y}, \mathbf{u}; \mathbf{p}) \\ \text{subject to } &\dot{\mathbf{x}} = \mathbf{f}(\mathbf{x}, \mathbf{u}; \mathbf{p}) \\ &\mathbf{y} = \mathbf{g}(\mathbf{x}) + \epsilon \\ &\mathbf{c}(\mathbf{x}, \mathbf{u}, \mathbf{p}) \leq \mathbf{0}\end{aligned}\quad (2)$$

where, J is a cost function representing the therapy goals (e.g., maximize sensorimotor recovery, while minimizing therapy time, effort, and cost). The function \mathbf{c} captures the set of general and subject-specific constraints (e.g., maximum cost affordable by the subject, constraints on daily therapy time and intensity, etc.). One could, in principle, solve this problem using tools from optimal control theory employing numerical approaches [29], provided the complete knowledge of \mathbf{f} and \mathbf{g} and nature of ϵ are available. Isolated models of selected sensorimotor learning processes exist for simple laboratory based movements, for example, sensorimotor adaptation [30], use-dependent learning [31], etc. However, currently no mechanistic models of sensorimotor learning or recovery exist that can be exploited for neurorehabilitation. Comprehensive models integrating different learning processes [32–34] and general contexts [35], accounting for subject-specific co-variables, and therapy parameters, are lacking. We also are unlikely to have such a detailed mechanistic model with high temporal resolution in the near future. However, this model in Eq. 1 is a useful way to conceptualize and contemplate the general recovery process in neurorehabilitation. A simpler approach to coupled non-linear differential equations (Eq. 1) for capturing causal relationships that can predict the effects of interventions is a structural causal model (SCM) [36], which can be learned from data and experiments.

3. Structural Causal Model of Robot-Assisted Therapy

A directed acyclic graph (DAG) representing the proposed SCM for RAT is shown in Figure 1, with its relevant variables (as nodes), along with their causal relationships (directed edges). We will refer to this model as the RAT-SCM in the rest of the paper. When examining the SCM presented in Figure 1, several fundamental questions emerge: What phenomenon does this model capture? Where is it applicable? What do the different nodes of the DAG represent? What are the mechanistic processes associated with the hypothesized causal links connecting these nodes? We will address these questions in the following subsections.

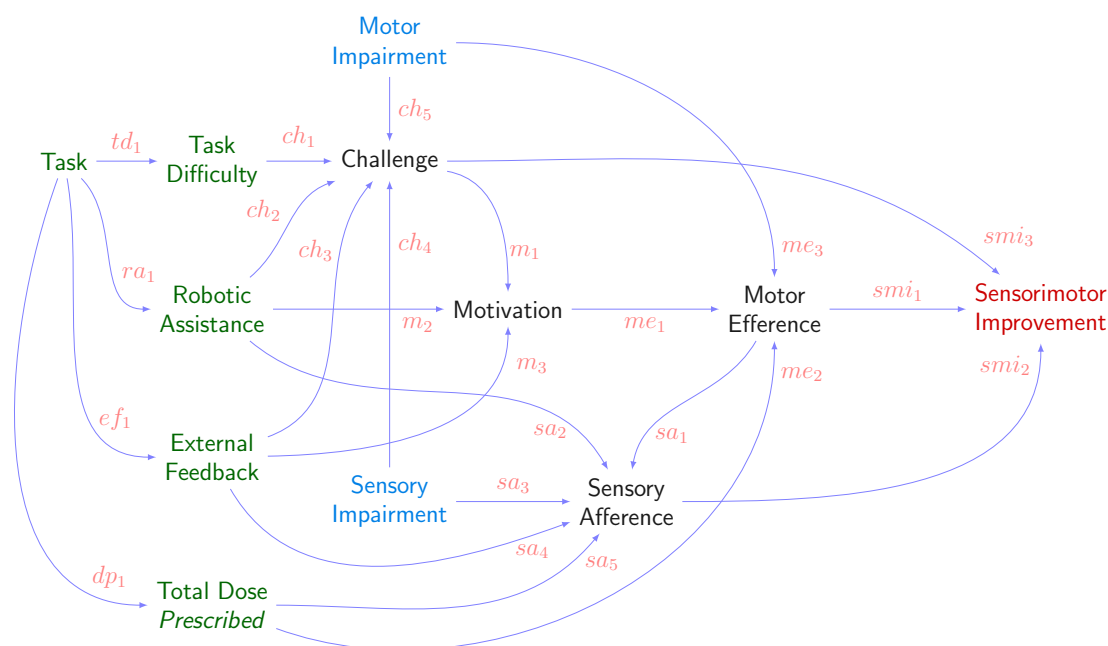


Figure 1. A directed acyclic graph representing the structural causal model of robot-assisted therapy. The colored nodes represent the type of node they are: red for target, green for ingredients, gray for mechanism nodes, and blue for subject-specific traits. The directed edges represent the known or hypothesized causal relationships between these nodes.

3.1. The Phenomenon Modeled by the RAT-SCM

“All models are wrong, but some are useful.”

— George E. P. Box

Three key properties should be noted to understand the scope of the proposed RAT-SCM. First, it is **high-level abstraction of the general dynamic model** described by Eq. 1. Second, it represents a **forward pass of the general recovery model** over a **fixed time interval** with **fixed therapy parameters**. Third, the model parameters are **robot-specific**; the overall model however represents the general RAT-driven recovery process. We elaborate on these properties below.

Subscribing to *treatment theory* [24,37], rehabilitation treatments can be separated into three components [24]: (a) *target* – the specific aspect of a subject’s behavior or function that is intended for change through the treatment; (b) the *treatment ingredients* that are administered to change the target of interest; and (c) the *mechanism of action* through which the treatment ingredients change the intended target; these are known or hypothesized causal connections between the ingredients and the target(s). This tripartite structure is contained in the SCM in Figure 1. The red-colored node represents the treatment target, and the green-colored nodes denotes the ingredients of RAT. The gray- and blue-colored nodes are factors associated with the mechanism of action of RAT. The connections

between this tripartite structure of treatments, the RAT-SCM in Figure 1, and the general recovery model represented by Eq. 1 is tabulated in Table 1. In the context of the RAT-SCM, we will at times refer to these three different node types collectively as target, ingredient, or mechanism nodes for simplicity.

Table 1. Connection between the tripartite structure of treatments, the RAT-SCM (Figure 1), and the detailed general recovery model (Eq. 1). The nodes of the SCM are highlighted in italic in the second column.

Treatment Theory	Robot-assisted Therapy SCM	General Recovery Model
Target	<i>Sensorimotor Improvement</i>	y
Ingredient	<i>Task, Task Difficulty, External Feedback</i>	u
	<i>Dose Prescribed, Robotic Assistance</i>	f(x, u; p)
Mechanism of action	Directed edges between the different nodes	g(x; p)
	<i>Challenge, Motivation, Voluntary Effort</i>	x
	<i>Dose Actual, Sensory Afference</i>	p
	<i>Motor Impairment, Sensory Impairment</i>	

While Eq. 1 describes the recovery process with infinite temporal resolution, the RAT-SCM in Figure 1 captures the same process over a fixed time interval, referred to as the *training epoch* T . The training epoch could correspond to a single therapy session (e.g. 30 minutes), a few therapy sessions over a few days (e.g. 5 sessions over week), or few weeks of therapy (e.g. 4 weeks of therapy which is typical for clinical trials). This is equivalent to running a forward pass of Eq. 1 over the training epoch T with fixed intervention variables $\mathbf{u}(t) = \mathbf{u}_0$ (e.g., fixed total dose, task, robotic assistance, etc.), as follows,

$$\begin{aligned} \mathbf{x}(t_0 + T) &= \mathbf{x}(t_0) + \int_{t_0}^{t_0+T} \mathbf{f}(\mathbf{x}(\tau), \mathbf{u}_0; \mathbf{p}) d\tau \\ \mathbf{y}(t_0 + T) &= \mathbf{g}(\mathbf{x}(t_0 + T); \mathbf{p}) + \epsilon \end{aligned} \quad (3)$$

where, t_0 is the start time of the therapeutic intervention, and $\mathbf{y}(t_0 + T)$ is the measured outcomes at the end of therapy at time $t_0 + T$. Note that the training epoch must be fixed and clearly specified for the RAT-SCM to learn its parameters from data, and to correctly interpret and use it.

Although, proposed as a general causal model of RAT, the specific model parameters of the RAT-SCM will differ between robots. The model parameters of the RAT-SCM fall into two categories: (a) the set of values assumed by the nodes, and (b) the functional forms and parameters associated with the directed edges between the nodes. These model parameters will differ between robots based on at least one of the following factors, which include the tasks supported by the robot, the nature of the robotic assistance implemented in the robot, and the nature and types of external feedback provided during training.

3.2. Components of the SCM

“Everyone knows what a curve is, until he has studied enough mathematics to become confused through the countless number of possible exceptions.”

— Felix Klein

The nodes of the DAG in Figure 1 are some of the key variables/factors in the RAT-driven recovery process that influence the treatment outcome. The choice of these factors is based on the current literature and our understanding of sensorimotor recovery process. In the following subsections, we will provide definitions for each of these variables, to the extent currently possible. These definitions

will focus on the nature of these variables, and more importantly, how these can be quantified and measured. Some of these definitions should be treated as working definitions, subject to refinement as our understanding of RAT matures. For each of these nodes we will also describe their known or hypothesized causes and effects as represented by the directed edges in the DAG. We will represent the variables corresponding to these nodes as X_i , where i will be uppercase alphabet of the node's name (e.g. the task node will be X_T , task difficulty will be X_{TD}). We will use the symbol \mathbf{Pa}_i to represent the set of parent nodes of X_i (nodes that have a direct arrow pointing to X_i), and we will use $\mathcal{F}_i(\bullet)$ to represent the function representing the causal relationship between X_i and its parents \mathbf{Pa}_i . Finally, we will use U_i to represent the exogenous noise [38] term associated with X_i , which captures the unmeasured causes of X_i and the random variability in X_i that is not explained by its parents \mathbf{Pa}_i .

3.2.1. Task

The type of movements trained, along the joints and limb segments involved, influence the nature and amount of sensorimotor outcomes. The task node captures the information about the movements prescribed for training as part of RAT during the training epoch.

Definition 1 (Task). *Task X_T is the specific movement types, involving a specific set of joints/limb segments, that a patient is prescribed during the training epoch.*

Causes and Effects. *As a root node of the DAG (Figure 1), task has no parents ($\mathbf{Pa}_T = \emptyset$). It directly determines the four other ingredient nodes: Task Difficulty, External Feedback, Robotic Assistance, and Total Dose Prescribed.*

The task X_T is a robot-specific node taking on values on a nominal scale consisting of the set of distinct movement-types \mathbb{T} supported by the given robot. We refer to this as the *task set* \mathbb{T} ,

$$\mathbb{T} = \{t_i \mid i = 1, \dots, n_T\}$$

where, t_i is the i^{th} movement-type supported by the robot and n_T is the total number of different movement types; both these are robot-dependent. For example, MIT-MANUS [39] - an end-effector robot - training only discrete point-to-point multi-joint arm reaching movements will have $n_T = 1$. There is no canonical approach to identify and categorize distinct movement-types supported by a robot. Thus, the classification of distinct movement-types may not always be clear. For instance, the BONES [40,41] - an exoskeleton robot - can train multi-joint (shoulder and elbow) and single joint (shoulder or elbow) discrete point-to-point reaching movements. Thus, in this case $n_T = 3$ would be a reasonable choice. However, one could argue that $n_T = 1$ for the BONES robot because multi-joint and individual joint training have similar therapeutic effects [42] and thus, from the recovery perspective, they need not be considered as distinct movement-types. However, a safer approach might be to use anatomical basis for task classification, while accounting for their similar therapeutic effects through the downstream causal links and their parameters.

For a robot with task set \mathbb{T} supporting $n_T > 1$ tasks, a subject might be prescribed to train a subset of these tasks during the training epoch. The value of the task node could be represented by binary n_T -vector $X_T = [X_{T,1} \ X_{T,2} \ \dots \ X_{T,n_T}]^T \in \mathbb{B}^{n_T}$, where the j^{th} element $X_{T,j}$ indicates if specific task $t_j \in \mathbb{T}$ is prescribed. For instance, PLUTO [2] - a modular, multifunctional hand robot - can train discrete point-to-point reaching movements involving the wrist flexion/extension (t_1), wrist ulnar/radial deviation (t_2), forearm pronation/supination (t_3), and hand opening/closing (t_4); thus, $n_T = 4$. If a subject is prescribed to train two movement types, namely, wrist flexion/extension and hand opening/closing, then the task node would be presented as $X_T = [1 \ 0 \ 0 \ 1]^T$.

3.2.2. Task Difficulty

Task difficulty could be thought of as the information processing and execution demands required to perform a prescribed task/movement. [43] divide task difficulty into two broad categories: *nominal* and *functional* task difficult. *Nominal difficulty* is the inherent demands of a task, independent of the performer and the environment. In the context of RAT-SCM, we define task difficulty as a restricted form of nominal difficulty of tasks performed during RAT without any physical assistance and augmented feedback.

Definition 2 (Task Difficulty). *Task difficulty X_{TD} is the nominal difficulty associated with a task performed with the robot without any physical assistance or augmented feedback.*

Causes and Effects. *Task difficulty is directly determined by its single parent - task $\mathbf{Pa}_{TD} = \{X_T\}$, and directly influences the Challenge node in the DAG.*

Each task $t_i \in \mathbb{T}$ has a set of parameters defining its spatiotemporal constraints, which determine its task difficulty. Task difficult can be captured by a non-negative real number \mathbb{R}_+ , where increasing values indicate increasing task difficulty. For instance, a planar point-to-point discrete reaching movement t_i has several parameters, including, the total number of targets, their spatiotemporal locations, the order of target appearance, etc. The task difficult of t_i is determined by these parameter values. For instance, target located closer to the subject would have lower task difficult than farther targets, targets appearing a fixed order would have lower difficulty than the ones appearing in a random order.

For a given task set \mathbb{T} and task prescription $X_T \in \mathbb{B}^{n_T}$ (see Section 3.2.1), the task difficult vector $X_{TD} = [X_{TD,1} \ X_{TD,2} \ \cdots \ X_{TD,n_T}]^T \in \mathbb{R}_+^{n_T}$, where $X_{TD,j}$ is the task difficulty of task $t_j \in \mathbb{T}$, defined as,

$$X_{TD} \leftarrow \mathcal{F}_{TD}(\mathbf{Pa}_{TD}, U_{TD}), \quad X_{TD,j} = X_{T,j} \cdot f_{TD,j}(\boldsymbol{\pi}_j) \quad (4)$$

where, $X_{T,j}$ indicates if t_j is prescribed, $\boldsymbol{\pi}_j \in \mathbb{R}^{m_j}$ are the parameters defining the spatiotemporal constraints of t_j , $m_j \in \mathbb{Z}_+$ is the number of parameters for the task t_j , and $f_{TD,j} : \mathbb{R}^{m_j} \rightarrow \mathbb{R}_+$ is the function that maps the task parameters of t_j to task difficulty. Note, that in Eq. 4 task difficulty is zero when a task is not prescribed.

3.2.3. External Feedback

Feedback is essential for motor learning and recovery [44], having both informational and motivational roles in the process [45,46]. The *external feedback* node refers to any additional, augmented, or enriched feedback provided to the subject during RAT. This includes, (a) visual and auditory feedback through gaming, virtual or augmented reality, (b) haptic feedback through the robot or external tendon vibration [47], (c) neuromuscular electrical stimulation (NMES) of motor and sensory structures [48], and (d) social, verbal or non-verbal feedback from a therapist or a caregiver interacting with the subject during therapy. Note that this feedback is over and above the intrinsic feedback (e.g., proprioceptive, tactile, visual etc.) naturally available to the subject during movement execution[45].

Definition 3 (External Feedback). *External feedback X_{EF} is any augmented task-related feedback provided to the subject during RAT. This is information that is not naturally available to the subject during movement execution.*

Causes and Effects. *External feedback is directly determined by its single parent - task ($\mathbf{Pa}_{EF} = \{X_T\}$), and directly influences three other nodes in the DAG: Challenge, Motivation, and Sensory Affference.*

There is no canonical way to quantify and faithfully represent the multidimensional construct of external feedback. A rudimentary approach is to use a binary variable indicating the presence or

absence of any augmented feedback during RAT. However, such a non-specific approach will club multiple dimensions of the feedback into a single variable, thus increasing response heterogeneity and masking causal effects. A more nuanced approach is to provide a detailed specification of the external feedback provided during RAT. Feedback could be decomposed into its distinct components and then quantified based on the type and amount of each of these components. These distinct components could include different sensory modalities (e.g., visual, auditory, or haptic) [49], feedback schedules (e.g., concurrent, terminal, faded, bandwidth etc.) [45], feedback content (e.g., knowledge of results, knowledge of performance etc.) [45], and social feedback (e.g., verbal praise, encouragement, etc.) [50]. This multidimensional information about the external feedback for a prescribed task t_j can be represented as a vector $\phi_j \in \mathbb{R}^{n_F}$. The components of the vector ϕ_j could indicate the amount of the different distinct feedback components in the external feedback provided during training for the task t_j ; n_F is the number of parameters used to capture the details of this external feedback. The overall external feedback provided for the full set of tasks could then be represented by a matrix of parameters $\Phi \in \mathbb{R}^{n_T \times n_F}$, where the rows corresponding to the prescribed tasks could have non-zero parameter values, while the rows corresponding to the non-prescribed tasks would be zero $\mathbf{0}^\top \in \mathbb{R}^{n_F}$.

3.2.4. Robotic Assistance

The most characteristic feature of RAT is the physical human-robot interaction during therapy, which can take different forms (assistive, resistive, counterbalance, error-augmentation, etc.) [51]. In the RAT-SCM, we will restrict our attention to the assistive form of physical interaction, where the robot applies external forces/torques on the human limb to augment voluntary movements. The assistance from the robot allows the subject to produce: (a) larger movements by moving the limb outside its active range of motion, and (b) faster movements than is possible voluntarily. Any physical interaction will qualify as robotic assistance only if the direction of the interaction forces/torques is aligned with the direction of the desired movement, i.e., $\mathbf{f}^\top \mathbf{v} > 0$, where \mathbf{f} is the generalized force vector and \mathbf{v} is the generalized velocity vector in the direction of the desired movement. The *robotic assistance* node captures the amount of this form of physical interaction provided during RAT.

Definition 4 (Robotic Assistance). *Robotic assistance is the physical human-robot interaction during RAT that augments voluntary movements by enabling larger and faster movements, along with completion of tasks not possible voluntarily.*

Causes and Effects. *Robotic assistance is directly determined by its single parent - task ($\mathbf{Pa}_{RA} = \{X_T\}$), and directly influences three other nodes in the DAG: Challenge, Motivation, and Sensory Afference.*

We can capture robotic assistance for a task t_j as a non-negative real number \mathbb{R}_+ . The amount of robotic assistance provided during therapy depends on three factors: (a) the task to be completed, (b) the magnitude of force/torque applied by the robot, and (c) the subject's physical effort in completing the task. When a subject is performing a task t_j with robotic assistance, the resulting movement $\mathbf{x}(t)$ is generated by the combined effect of the subject's active effort $\mathbf{h}(t)$ and the robotic forces/torques $\mathbf{f}(t)$. With the knowledge of \mathbf{h} and \mathbf{f} , we can define the amount of robotic assistance as the following,

$$a = \frac{\|\mathbf{f}(t)\|}{\|\mathbf{h}(t) + \mathbf{f}(t)\|} \in \mathbb{R}_+ \quad (5)$$

It is assumed that voluntary effort $\mathbf{h}(t)$ is also expressed a forces or torques. According the above definition, (a) $a = 0$, when the task is completed with no robotic assistance $\mathbf{f}(t) = \mathbf{0}$, and (b) $a = 1$ when the task is completed with no active voluntary effort from the subject $\mathbf{h}(t) = \mathbf{0}$. Note that Eq. 5,

the denominator is the overall “input” that produces the movement “output” $\mathbf{x}(t)$. In principle, the denominator could be computed through an inverse model of the human-robot dynamics, as follow,

$$\mathbf{h}(t) + \mathbf{f}(t) = \mathcal{H}^{-1}(\mathbf{x}(t); t_i) \implies a = \frac{\|\mathbf{f}(t)\|}{\|\mathcal{H}^{-1}(\mathbf{x}(t); t_i)\|} \quad (6)$$

One such approach using the cross-correlation between actual and simulated trajectories, based on an estimated dynamic model of the human arm, is used as a measure of “slacking” [52], which provides an indirect measure of the amount of assistance.

The overall robotic assistance provided for the full set of tasks could be represented by a vector $X_{RA} = [X_{RA,1} \ X_{RA,2} \ \cdots \ X_{RA,n_T}]^T \in \mathbb{R}_+^{n_T}$, where the elements corresponding to the non-prescribed tasks would be zero.

3.2.5. Total Dose Prescribed

Total dose prescribed refers to the total amount of therapy prescribed to the subject during the training epoch. [53] define ‘total dose’ as the product of dose and dosage defined similarly to their definitions in pharmacological interventions [53]. *Dosage* is multidimensional, consisting of therapy session frequency and the total duration of therapy [53]. *Dose* is also treated as multidimensional construct [54], consisting of therapy intensity and the duration of an intervention session [53]. *Intensity* is defined as the amount of physical or mental effort put forth by a subject during therapy [53], which is not easy to quantify [53].

Definition 5 (Total Dose Prescribed). *Total dose prescribed* X_{TDP} is the total active therapy time prescribed to the subject during the training epoch for the prescribed tasks.

Causes and Effects. *Total dose prescribed* is directly determined by its single parent - task ($\mathbf{Pa}_{TDP} = \{X_T\}$), and directly influences two nodes in the DAG: *Motor Efference*, and *Sensory Afference*.

In the definition for “total dose prescribed”, we implicitly assume that the patient is 100% actively engaged in therapy. However, in practice the actual total dose received by a subject will be different from this value, depending on the actual training duration and his/her level of engagement during therapy. This actual total dose will have a motor and sensory component, which are captured by the *Motor Efference* and *Sensory Afference* nodes in the DAG (see Sections 3.2.10 and 3.2.11, respectively).

3.2.6. Motor Impairment

According to the International Classification of Functioning, Disability and Health [55], an *impairment* is defined as problem in the body structure or function such as a deviation or a loss. *Motor impairment* refers to impairments to the neuromuscular system impacting one’s ability to move.

Definition 6 (Motor Impairment). *Motor impairment* X_{MI} is the loss or abnormality of the neuromuscular anatomy or physiology that impacts one’s ability to produce skilled motor actions.

Causes and Effects. *Motor impairment* is a root node in the DAG, and thus has no parents ($\mathbf{Pa}_{MI} = \emptyset$). It directly influences two other nodes in the DAG: *Challenge*, and *Motor Efference*.

Motor impairment captures several low-level motor control parameters, which have been traditionally captured through standardized clinical scales (e.g., Fugl-Meyer Assessment [56] for stroke), and more recently through sensor-based measurements [57–59]. A generalized approach to capture motor impairments in the RAT-SCM is to represent it as a vector $X_{MI} \in \mathbb{R}^{n_M}$. Here, the individual elements of X_{MI} will represent different motor impairment parameters relevant to the specific clinical population being treated and the nature of the robot. For example, these could be the individual components of the FMA, joint range motion, joint strength, movement quality measures, etc. The

exact choice of the components of X_{MI} for the RAT-SCM will depend on various interrelated factors: the nature of the robot, the limb segments and the motor control parameters being targeted, and the clinical condition being treated.

3.2.7. Sensory Impairment

The sensory impairment node is the sensory equivalent of the motor impairment node, capturing anatomical and physiological damage to the sensory structures relevant for motor control and learning. Sensory impairments are considered to be an important factor influencing motor recovery [60].

Definition 7 (Sensory Impairment). *Sensory impairment X_{SI} is the loss or abnormality of the sensory anatomy or physiology that impacts one's ability to produce and learn skilled motor actions.*

Causes and Effects. *Sensory impairment is a root node in the DAG, and thus has no parents ($\mathbf{Pa}_{SI} = \emptyset$). It directly influences two other nodes in the DAG: Challenge, and Sensory Afference.*

Similar to motor impairment, sensory impairment is also multidimensional and several standardized clinical scales [60], and technology-assisted assessments exist [58,61–63]. Sensory impairment can also be captured through a vector $X_{SI} \in \mathbb{R}^{m_s}$; the exact scale choice depends on various interrelated factors.

3.2.8. Challenge

Challenge is believed to be a key driver of motor learning and recovery [43,64–66]. Although [43] do not provide an operational definition of challenge, their arguments suggest that challenge is effectively functional task difficulty - the relative difficulty of a task with respect to the skill level of the performer and the environmental conditions [43].

Definition 8 (Challenge). *Challenge X_C is the relative functional difficulty of a task with respect to the skill level of the performer and the environmental conditions.*

Causes and Effects. *Challenge is directly determined by five parent nodes in the DAG: Task Difficulty, External Feedback, Robotic Assistance, Motor Impairment and Sensory Impairment ($\mathbf{Pa}_C = \{X_{TD}, X_{RA}, X_{EF}, X_{MI}, X_{SI}\}$). It directly influences two other nodes in the DAG: Motivation, and Sensorimotor Improvement.*

Challenge or functional task difficulty shapes two important aspects of training: (a) the task-level “interpretable information” essential for the motor learning [43], and (b) the mental experience of the performer during training, involving mental workload, attention, motivation, etc. [65]. The challenge node in the DAG is a parsimonious representation of these two aspects of training.

There are five causal arrows converging onto the challenge node in the proposed RAT-SCM. The nature of these causal influences are as follows: (i) Task Difficulty (ch_1): higher nominal difficulty increases challenge [43], (ii) Robotic Assistance (ch_2): assistance can decrease challenge for a given task, (iii) External Feedback (ch_3): appropriate feedback can decrease challenge, (iv) Sensory Impairment (ch_4) and Motor Impairment (ch_5): greater impairment increases challenge. Note that these relationships are likely to be non-linear and some non-monotonic.

Challenge is a latent construct and thus is not directly measurable; in Table 1 challenge is equated to an internal state variable in the general recovery model. However, there are several potential indirect measures of challenge. The interpretable information aspect of challenge can be measured through performance variables such as a success rate, task error, movement variability, etc.; the exact choice of the performance measure will depend on the task being trained. The mental experience aspect can be measured through subjective questionnaires such as the NASA Task Load Index [67], which measures the mental workload experienced by a subject performing a task. More objective measures of mental experience include the enzymatic activity of the salivary α -amylase [68] - a biomarker of the activity of the sympathetic nervous system, reaction time during dual-tasking [68], electroencephalography

(EEG)-based measures [69], etc. Challenge can be represented as a non-negative real number \mathbb{R}_+ . Thus, the challenge node in the RAT-SCM could be represented as a vector $X_C \in \mathbb{R}_+^{n_T}$, a single number for each of the tasks.

$$X_C \leftarrow \mathcal{F}_C(\mathbf{Pa}_C, U_C), \quad X_{C,j} = f_{C,j}(X_{TD,j}, X_{RA,j}, X_{EF,j}, X_{MI}, X_{SI}, U_{C,j}) \quad (7)$$

where, $f_{C,j}$ is function that computes the challenge for a task t_j given the value of the variables in \mathbf{Pa}_C . The function $f_{C,j}$ will assign $X_{C,j} = 0$ when t_j is not prescribed, i.e., $X_{TD,j} = 0$ (see Section 3.2.2).

3.2.9. Motivation

The OPTIMAL theory [50,70] proposed by Wulf and Lewthwaite emphasizes the importance of motivation in motor performance and learning. Motivation and its associated factors are believed to influence motor learning processes [71], and its role in patient outcomes are also well supported in the neurorehabilitation literature [50,72–74]. Motivation for neurorehabilitation is a highly dynamic [73, 74] and complex construct [75] influenced by: (i) factors intrinsic to the subject (e.g., personality, psychological status, depression, anxiety etc.), (ii) extrinsic factors (e.g., family and social support), (iii) disease severity and cognitive deficits, and (iv) factors related to the nature and content of the neurorehabilitation intervention. The last factor is the most relevant in the context of the RAT-SCM.

Definition 9 (Motivation). *Motivation X_M is an internal state of a subject that drives behavior towards the goal of attaining functional recovery through neurorehabilitation.*

Causes and Effects. *Motivation is directly determined by three parent nodes in the DAG: Challenge, Robotic Assistance, and External Feedback ($\mathbf{Pa}_C = \{X_C, X_{RA}, X_{EF}\}$). It directly influences one node in the DAG: Motor Efference.*

The self-determination theory proposed by [76] broadly differentiates motivation into two categories: intrinsic and extrinsic. Intrinsic motivation drives activities for their inherent satisfaction; it is more desirable [76] for improved therapy adherence. While, extrinsic motivation regulates activities through external rewards or punishments, and comes in several forms with some forms being more desirable than others [76]. The choice of appropriate levels of challenge, optimal robotic assistance, and the right type and amount of external feedback can build competence, autonomy, and relatedness – the three basic psychological needs identified by the self determination theory [76] to be conducive for intrinsic motivation for therapy.

Motivation and challenge have been shown to have an inverted U-relationship [69,77,78] with low challenge leading to boredom and high challenge leading to anxiety and frustration; both these extremes are detrimental to motivation. Thus, optimal challenge not only contains the maximal interpretable information for motor learning [43], but also maximizes intrinsic motivation [65]. Robotic assistance has been shown to increase motivation compared to unassisted training after controlling for success rate [79]; this supports the direct causal link between robotic assistance and motivation. External feedback can influence motivation through several means: (a) augmented audiovisual feedback through gaming, virtual or augmented reality can enhance motivation [74] by making therapy enjoyable, and (b) appropriately designed/scheduled task-related feedback can enhance motivation through increase perception of competence and self-efficacy [80]. For example, providing feedback after successful trials has been shown to increase motivation [81]. A recent multi-center survey on motivational factors in rehabilitation, the positive achievement emotions and self-efficacy was identified to be top motivational factor by both patients and clinicians [82].

Motivation is commonly measured through self-reported questionnaires, such as the intrinsic motivation inventory [79], stroke rehabilitation motivation scale [73], motivation for rehabilitation scale [83], etc. Administering such questionnaires is not feasible on a regular basis to dynamically track the motivation levels of patients during therapy. In such scenarios, a visual analogue scale or 0–10

numerical scale could be employed as a coarse measure of motivation. Motivation levels for specific tasks might also be inferred from task adherence during therapy, with the assumption that higher adherence is indicative of higher motivation for that task. Similar to challenge, motivation can also be represented as a vector in $X_M \in \mathbb{R}^{n_T}$.

3.2.10. Motor Efference

Active voluntary participation [65,84] and sufficient dose [53,85] are two necessary, and arguable most important, ingredients for motor learning and recovery. The motor efference node captures this key information in the RAT-SCM that has a direct impact on recovery.

Definition 10 (Motor Efference). *Motor efference X_{ME} is the total physical and mental effort exerted by the patient during therapy over the training epoch.*

Causes and Effects. *Motor efference has three parent nodes: Motor Impairment, Motivation, and Total Dose Prescribed ($\mathbf{Pa}_{ME} = \{X_{MI}, X_M, X_{TDP}\}$). It influences two nodes: Sensory Afference, and Sensorimotor Improvement.*

The causal link me_1 from motivation to motor efference capture the intensity of training, which was defined by [53] as the amount of physical or mental work exerted by the patient during movement training. Increasing levels of intrinsic motivation is likely to increase both the intensity as well as adherence to training [86–88]. Attentional resources may act as a confounder in the recovery in subacute stroke [89]; attention during therapy is likely to be positively influenced by motivation. Adherence or the total actual therapy duration will be influenced by the total dose prescribed, which is captured by the causal link me_2 . Finally, the actual motor output produced during training will also be influenced by the motor ability of the subject. More severely impaired patients produce smaller, slower, and poorly coordinated movements compared to mildly impaired patients; this is captured by the me_3 causal link.

Motor efference can be represented as a vector $X_{ME} \in \mathbb{R}_+^{n_T}$ consisting of the motor efference for the individual tasks.

$$X_{ME} = \left[X_{ME,1} \quad \cdots \quad X_{ME,n_T} \right]^T \leftarrow \mathcal{F}_{ME}(\mathbf{Pa}_{ME}, U_{ME}) \quad (8)$$

where, $X_{ME,j}$ is the motor efference for task t_j . The individual motor efferences for each task could be computed as the product of the individual causal effects of its three parents, as the following,

$$X_{ME,j} = f_{ME_1}(X_{M,j}) \cdot f_{ME_2}(X_{TDP,j}) \cdot f_{ME_3}(X_{MI}) \quad (9)$$

where, $f_{ME_1}(\bullet)$, $f_{ME_2}(\bullet)$, and $f_{ME_3}(\bullet)$ capture the functional relationship of the causal effect of motivation, total dose prescribed, and motor impairment on motor efference, respectively.

The causal link $f_{ME_2}(\bullet)$ is probably the easiest to model. This could be the total time spent training task t_j with the robot. If the task t_j is not prescribed, this function returns 0, to indicate that t_j was not trained, else it could return a non-negative number. The other two causal links are harder to model. There is currently no standard approach to measure the intensity of neurorehabilitation training [53]. A potentially useful behavioral correlate could be movement vigor - a heterogeneous construct related to the velocity or duration of a movement relative to its extent [90]. Faster movements to a target indicate increased subjective value associated with the target [91], signaling heightened motivation. Faster movements require higher physical effort, and possibly higher mental effort to ensure accuracy to mitigate signal-dependent noise [92]. However, such behavioral measures of intensity/effort will need to be normalized to account for the nature of a task, and subject-dependent factors, such as age, gender, weakness, etc. [53]. Other physiological measurements that could be employed for this purpose include skin conductance [93], error-related potentials in EEG [94], salivary α -amylase activity [68], etc. However, not all such measurements may be practical for routine use.

3.2.11. Sensory Afference

Sensory feedback is vital for movement planning, execution, and learning [95]. Any movement training will generate sensory signals that ascend back to the central neural structures shaping movement performance and learning. This can involve any of the four sensory modalities: somatosensory, vision, auditory, and vestibular.

Definition 11 (Sensory Afference). *Sensory Afference X_{SA} is the total quantity and quality of sensory feedback provided to the subject during therapy over the training epoch.*

Causes and Effects. *Sensory afference has five parent nodes: Robotic Assistance, Sensory Impairment, External Feedback, Total Dose Prescribed, and Motor Efference ($\mathbf{Pa}_{SA} = \{X_{ME}, X_{SI}, X_{EF}, X_{RA}, X_{TDP}\}$). It influences one node: Sensorimotor Improvement.*

The quantity of sensory feedback refers to the cumulative magnitude of sensory stimulation (e.g., area under the sensory stimulation magnitude curve). Quality, on the other hand, refers to a measure of congruence or alignment between the intended task and the sensory feedback provided during task performance. Thus, sensory afference can be thought of as the total amount of “task-aligned” sensory feedback provided during therapy over the training epoch. We can represent sensory afference as a vector $X_{SA} = [X_{SA,1} \ X_{SA,2} \ \cdots \ X_{SA,n_T}]^T \in \mathbb{R}^{n_T}$ of real numbers; unlike motor efference we could allow sensory afference to assume negative values to indicate anti-correlated sensory feedback. The sensory afference $X_{SA,j}$ for a given task t_j could be computed as the following over the training epoch T ,

$$X_{SA,j} = f_{SA_3}(X_{SI}) \cdot \left(\int_T \hat{\phi}_j(t)^T \mathbf{W} \phi_j(t) dt \right) \quad (10)$$

where, $f_{SA_3}(\bullet)$ captures the causal effect of the sensory impairment on the sensory afference. The second term computes the total “task-aligned” sensory feedback while training task t_j over the training epoch. $\hat{\phi}_j(t), \phi_j(t) \in \mathbb{R}^{n_F}$ are vector functions of time over the interval $(0, T)$ representing the expected and actual sensory feedback for the task t_j . \mathbf{W} is a positive definite matrix representing the weights for the different sensory feedback components.

Sensory feedback during training can be generated and moderated by various factors. The causal link sa_1 represents the sensory feedback generated by the voluntary movement performed by the subject. Robotic assistance can produce larger and faster movements than that produced by pure volition, and can thus result in augmented sensory feedback (sa_2). A robot applies external forces on the limb segment, which activates the spindle and Golgi tendon afferents of the antagonistic muscles, along with other joint afferents and some somatosensory afferents at the point of application of the force. A wide range of sensory feedback can be provided through the causal link sa_4 from the external feedback node. These could include, NMES which can activate a range of sensory and motor structures [48] beyond what is possible with robotic assistance, muscle tendon vibration [47], augmented visual or auditory feedback [96], etc. The causal link sa_5 will play a role in determining the actual dose of sensory feedback provided during therapy, similar to its influence on motor afference (me_2). The effect of these four causal links (sa_1, sa_2, sa_4, sa_5) could be represented by the integral term in Eq. 10. The quantity and quality of this sensory feedback will be moderated by the subject’s level of sensory impairment, indicated by the causal link sa_3 ; this is represented by f_{SA_3} in Eq. 10. This is similar to the moderating effect of motor impairments on motor afference (me_3).

3.2.12. Sensorimotor Improvement

The *Sensorimotor Improvement* node is the outcome or the target node of the RAT-SCM that captures the change in the subject’s sensorimotor behavior undergoing RAT. In their paper on the rehabilitation treatment specification system, [24] proposed that the targets must be specific proximal changes

expected from a treatment. Thus, given the nature of RAT, the sensorimotor improvement node will be restricted to measurements of impairment and low-level motor control variables.

Definition 12 (Sensorimotor Improvement). *Sensorimotor Improvement X_{SMI} is the change in low-level motor control and impairment level variables of a subject undergoing RAT over the given training epoch.*

Causes and Effects. *Sensorimotor improvement has three parent nodes: Motor Efference, Sensory Afference, and Challenge ($\mathbf{Pa}_{SMI} = \{X_C, X_{ME}, X_{SA}\}$).*

RAT can lead to improvements in various impairment-level and motor control variables. These include improvements in joint range of motion [97,98], movement speed [99,100], reaching accuracy [100], movement smoothness [99,100], path efficiency of arm reaching movements [100], grip strength [98], etc. These are usually measured using sensor-based systems or robots. In addition to this, there is also good evidence supporting the improvement of UL impairments after RAT in stroke as measured by the FMA [8]. The sensorimotor improvement node captures the change in these variables over the training epoch, which can be represented as a vector $X_{SMI} \in \mathbb{R}^{n_O}$, where n_O is the number of impairment/motor control variables targeted by the robot. Note that these impairment measurements can include joints not directly trained during therapy, to account for the generalization of therapeutic gain to the proximal UL when training the distal UL [101].

The combined effect of the three causal links si_1 , si_2 , and si_3 on the sensorimotor improvement node can be represented as,

$$X_{SMI} \leftarrow \mathcal{F}_{SMI}(\mathbf{Pa}_{SMI}, U_{SMI}) \quad (11)$$

where, \mathcal{F}_{SMI} represents the causal mechanism determining X_{SMI} given \mathbf{Pa}_{SMI} . The function \mathcal{F}_{SMI} will be a highly complex, non-linear map that captures the multitude of motor learning processes at play during therapy [32,43,65,102]. The motor efference X_{me} and sensory afference X_{sa} nodes drive these processes stimulating the central neuroplastic [32,71], and peripheral neuromuscular/soft tissue changes [103] that underlie sensorimotor improvements. The causal effects X_{ME} and X_{SA} on the central neuroplastic changes are likely to be moderated by internal brain states, such as experienced challenge [43,65,67] and motivation [50,65,104,105]. This is captured by the causal link si_3 .

4. Implications of the RAT-SCM

"Prediction is very difficult, especially about the future."

— Neils Bohr

The utility of any model is judged by the known phenomena it can explain and the testable predictions it makes about the world. In this section, we will highlight some of the phenomena associated with RAT explained by the proposed RAT-SCM, along with some predictions of the model, wherever applicable.

4.1. Slacking in RAT

Slacking is a commonly observed phenomenon in RAT, where the human subject reduces his/her effort when there is more than the required robotic assistance to complete a given task [106]. In the RAT-SCM, high levels of robotic assistance can reduce challenge, which in turn reduces motivation, and thus motor efference (or effort). [107] provide some support to the negative impact of slacking on the change in motor impairments, as measured using the FMA. Fitting a linear state space model to data from a RAT clinical study, they found that the estimated parameter for the slacking term was correlated to the change in the FMA score for the individual subjects; subjects displaying more slacking had smaller gains in motor impairment [107]. In the extreme case, maximal slacking results in purely passive movements, that do not produce any appreciable improvements in motor function or impairments [108]. In the RAT-SCM, passive movements would have zero challenge and motor

efference (no voluntary effort), thus resulting in no appreciable sensorimotor improvement; changes to peripheral soft tissue might still happen [103].

4.2. Effect of Augmented Sensory Feedback

There is evidence to support the positive effects of augmented external feedback on the recovery of motor impairments of the UL post-stroke [109]. A recent meta-analysis comparing the effect of BCI-triggered assisted training with robots or NMES found that BCI+NMES had significantly large improvements in motor function compared to BCI+Robots [110,111]. This could be attributed to the differences in the nature and amount of sensory feedback resulting from NMES compared to robots. NMES produces larger activation of the sensory efference node in congruence with motor efference generated through voluntary effort, thus resulting in larger sensorimotor improvement. Both robotic and NMES assistance activate the spindles and the Golgi tendon organs of the antagonists. However, NMES additionally activates the agonists, the cutaneous sensory structures below the electrodes, and other sensory nerves along the path of the electrical current. Another recent study employing tendon vibration in conjunction with RAT demonstrated larger benefits for the tendon vibration group than the one without [47]. This too can be explained as the consequence of increased sensory efference in the RAT-SCM.

4.3. Effect of Initial Impairments

The baseline impairment plays a moderating role on the amount of improvement following RAT [112,113]. Similar moderating effects have been identified for baseline sensory impairments on gains made from RAT [16,19]. These observations can be explained by two causal routes in RAT-SCM. Impairments have a moderating effect on the motor efference (Eq. 9) and sensory efference (Eq. 10) during therapy, which in turn impact sensorimotor impairment. The levels of impairments could also limit the levels of challenge and motivation achievable through RAT, and thus impact recovery. For instance, a severely impaired subject might find training challenging even with high levels of assistance.

4.4. Effect of Robotic Assistance

The role of robotic assistance in sensorimotor recovery has been a topic of interest since the early days of RAT [114,115]. Surprisingly, only a handful of studies have investigated this issue while controlling for the relevant confounders. Our recent meta-analysis evaluating such studies found that robotic assistance has a significant effect (standardized mean difference ≈ 0.4) on motor impairments with similar effects on both arm and hand training [116]. The small overall sample size (≈ 300) and moderate heterogeneity ($I^2 \approx 70\%$) of these studies mean these results have to be treated with caution. However, this result warrants future systematic evaluation of the clinical value of robotic assistance.

The proposed RAT-SCM model predicts that the presence of robotic assistance will result in better outcomes than unassisted training. This causal effect on sensorimotor improvement can be through: (a) enhanced motivation leading to more training [117] and (b) enhanced sensory efference; note that the third potential route from challenge to sensorimotor impairment has a moderating effect on the other two routes. The motivational route of robotic assistance on recovery is known [15,19,79,117]. The other and arguably more interesting route is the one through enhanced sensory efference engaging Hebbian-like learning mechanisms [15,118,119]. A recent study [19] found that the standard RAT leads to better outcomes only in patients with intact proprioception, lending some support to the existence of this sensory efference-mediated causal route. Another interesting prediction of the RAT-SCM is that NMES-assisted therapy will lead to better outcomes than RAT once we control for the task, task difficulty, external feedback, and total dose.

5. Limitations of the RAT-SCM

"The truth of the story lies in the details."

— Paul Auster

The RAT-SCM is the first attempt at a comprehensive model for the mechanistic understanding of RAT. It brings together most of the known important factors involved in RAT and proposes a set of causal links between them, mostly based on the existing literature. The chosen level of abstraction for the model strikes a balance between the specificity of the underlying mechanistic processes and the practical aspects, such as measurability of its individual factors, identifiability of causal links, and the model's clinical utility. The RAT-SCM, as currently specified, has important limitations that we make explicit in this section. A clear understanding of these limits is essential both for interpreting the model appropriately and for guiding future work aimed at refining and extending it.

Node definition and measurement. Many of the node definitions provided in the RAT-SCM are working definitions with little consensus from the field. Without agreed definitions, standardized measurement of these nodes will be difficult. It is wise to avoid premature definitions and avoid mistakes previously made in the field. For instance, movement smoothness - an important construct - was being quantified with inappropriate methods [120–122] for several years due to the lack of consensus on its definition and on what constituted a valid measure of smoothness. While striving to find an agreeable definition, a balance must be struck between the specificity of the construct and its routine measurability, preferably involving minimal manual processes.

Restrictions to assistive forms of robotic interaction. The proposed model is restricted to robotic assistance, while there are numerous other forms of physical human-robot interaction [51]. These include, counterbalance assistance [123], error amplification [124,125], active constrained assistance [126], resistive strategies [127], etc. The focus on robotic assistance was because this is the most common form of robotic interaction implemented in RAT. This restriction can be easily addressed by modifying the robotic assistance node through: (a) appropriate encoding and quantification of the different types of robotic interactions, and (b) modification of the functions corresponding to the causal links coming out of this node; for example, counterbalance assistance unlikely to enhance sensory afference, while error amplification and resistance might enhance sensory afference beyond assisted training. The impact on motivation is also likely to be different for the different types of interactions.

Lack of training-recovery loops. DAGs are by definition acyclical [38]. RAT is not a simple feedforward process; for instance a patient's current impairment level influences his/her recovery, which in turn changes his/her impairment level in the future. One way to address this issue is to unfold the DAG over time [38]. A different instance of the same DAG is considered for each training epoch, with causal arrows between consecutive training epochs. For example, the sensorimotor improvement at the time instant k will impact motor/sensory impairment at time $k + 1$; this corresponds to a causal arrow from the sensorimotor improvement node from time k to the motor and sensory impairment nodes in next time $k + 1$.

Lack of information about capacity to improve. [128] showed that stroke subjects with the same level of performance need not have the same capacity for improvement or learning. In particular, they found that the stroke subjects trained on a particular task are not the same as untrained ones with a lower impairment. Thus, impairment or performance levels alone are insufficient to determine improvement following an intervention. Its unclear how this information could be captured in the RAT-SCM. One possibility is to incorporate an additional node that captures the "learning reserve" or "learning capacity" of a subject. This node is likely to depend on the initial impairment after stroke (SAFE score or the presence of MEP) [20,21], and the history of intervention provided to the subject. However, the exact nature of this node and its measurement currently remain unknown.

Others. In addition to the aforementioned limitations, there are other limitations worth noting. (a) The proposed RAT-SCM is not complete in capturing all the relevant factors and causal links. Its likely that there other important factors not included in the DAG, along with missing or incorrectly specified causal links. For instance, the only two nodes capturing subject characteristics in the RAT-SCM are the motor and sensory impairments. Impairments are necessary but are most probably insufficient. A more realistic RAT-SCM will need to consider a detailed set of subject traits including, age, personality,

fatigue, cognitive impairments, neurophysiological parameters, social/family support etc. The causal effects of these subject traits will need to be incorporated to improve the validity of the RAT-SCM. (b) The model, its discussion, and the supporting literature are primarily focused on the UL RAT in stroke. The applicability of the model to other conditions and to the lower-limb will need to be carefully investigated by experts from those areas.

6. Using the RAT-SCM in Clinical Practice

“In theory there is no difference between theory and practice, while in practice there is.”

— The Yale Literary Magazine, 1882

Although, the proposed SCM is formulated as a general model of RAT-driven sensorimotor recovery, its details will be robot specific. The RAT-SCM model will need to be instantiated for a given robot (e.g., MIT-MANUS, PLUTO) and its parameters identified through data obtained from observations and experimental studies. These learned parameters will include, the functional relationships corresponding to the various causal links, and the distribution of the exogenous variables associated with the different nodes. For the sake of this section, we will assume that we have an accurate RAT-SCM for a particular neurological condition, which has been fully specified for a given robot. This causal model can be used for implementing precision neurorehabilitation. Given a particular patient with some characteristics and health-related parameters \mathbf{p} , along with a set of constraints and preferences \mathbf{c} for RAT, we can use the causal model to answer two important RAT planning questions, in the following order:

- **Q1.** What is the maximum expected treatment outcome for the given patient over the training epoch?
- **Q2.** What are the optimal set of therapy parameters (values for the ingredient nodes) that results in this maximum expected treatment outcome?

First, we would pose **Q1** taking into consideration the patient characteristics and constraints, which is an optimization problem over the RAT-SCM [129] searching over the space of parameter values of the ingredient nodes.

$$\begin{aligned} J^* = & \underset{\mathcal{X} \in \mathbb{X}}{\text{maximize}} && J(X_{SMI}, \mathcal{X}; \mathbf{p}) \\ & \text{subject to} && X_{SMI} = \mathcal{G}(\mathcal{X}, \mathbf{p}) \\ & && \mathbf{c}(\mathcal{X}, \mathbf{p}) \leq \mathbf{0} \end{aligned} \quad (12)$$

where, $\mathcal{X} = (X_T, X_{TD}, X_{RA}, X_{EF}, X_{TDP})$ is a tuple of the ingredient nodes. \mathbb{X} is the set of all possible values for tuple of ingredient nodes \mathcal{X} . The function $J(\bullet) : \mathbb{R}^{n_o} \mapsto \mathbb{R}$ computes the overall sensorimotor improvement from the X_{SMI} . $\mathcal{G}(\bullet)$ is the overall function capturing the causal mapping from the set of ingredient nodes and the patient characteristics to the sensorimotor impairment node. The constraints and preferences of the subject are captured by the vector function $\mathbf{c}(\bullet)$. The number J^* is the maximum expected sensorimotor improvement for the given subject characteristics \mathbf{p} and constraints \mathbf{c} .

If J^* - the answer to **Q1** - is sufficiently high, then prescribing RAT for the given subject would be deemed worthwhile. At this stage, we would query the model of the optimal value for the ingredient nodes that produces J^* .

$$\begin{aligned} \mathcal{X}^* = & \underset{\mathcal{X} \in \mathbb{X}}{\text{arg max}} && J(X_{SMI}, \mathcal{X}; \mathbf{p}) \\ & \text{subject to} && X_{SMI} = \mathcal{G}(\mathcal{X}, \mathbf{p}) \\ & && \mathbf{c}(\mathcal{X}, \mathbf{p}) \leq \mathbf{0} \end{aligned} \quad (13)$$

where, \mathcal{X}^* is the set of values for the ingredient nodes that can give us the maximum expected sensorimotor improvement J^* .

The above discussion is meant to only demonstrate how a causal model can be employed for rationally prescribing RAT for a given patient. The actual implementation of this process is contingent

on the availability of a fully specified RAT-SCM model, and the availability of appropriate constrained optimization algorithms over the causal DAGs [129].

7. Conclusion

The proposed RAT-SCM is timely because device development has far outpaced mechanistic understanding of RAT for UL neurorehabilitation. The SCM pinpoints to specific key variables identified from the UL RAT literature, along with the known/hypothesized causal links between them. This explicit, concrete, critique-able causal architecture allows principled reasoning about interventional arguments (e.g., effect of robotic assistance, dose), confounding variables, and mediating and moderating mechanisms (e.g., impact of initial impairments), thus enabling scientific discourse beyond associational and heuristic arguments (e.g., biomarkers correlated with recovery; see Section 1).

Nevertheless, the proposed RAT-SCM is provisional and necessarily incomplete (see Section 5). It is a useful, structured synthesis of our current understanding of RAT, and not a complete, unquestionable description. The model's components, its implications, and predicted conditional independencies must be challenged with evidence and consensus. Future observational and experimental studies, must take on the mantle of empirical falsification, refinement of the nodes and the causal edges, and the incorporation of the missing constructs (e.g., additional subject traits; see Section 5). Carefully designed multi-disciplinary expert consensus studies will be necessary for accurate and useful construct definitions, along with valid and practical measurement methods.

The clinical planning demonstration illustrates how, in theory, a fully specified RAT-SCM for a given robot and indication can support precision neurorehabilitation for individual patients. The proposed model provides a principled way to frame questions about the attainable outcomes under a given set of constraints, along with the therapy parameters for this optimal outcome.

In conclusion, this work is not a claim to a definitive mechanistic account of RAT, but an effort to put forth a tangible causal graph on the table for RAT-driven recovery. The hope is that this causal model will set off a cascade of systematic critique, empirical testing, and iterative revision by the neurorehabilitation, robotic rehabilitation, and causal-inference communities, moving the field towards shared, testable causal models that can genuinely inform the design and prescription of robot-assisted therapy.

Acknowledgments: I thank Mr Manigandan Chockalingam (University of Galway) for his insightful comments about the casual graph.

References

1. Maciejasz, P.; Eschweiler, J.; Gerlach-Hahn, K.; Jansen-Troy, A.; Leonhardt, S. A survey on robotic devices for upper limb rehabilitation. *Journal of neuroengineering and rehabilitation* **2014**, *11*, 3.
2. Nehrujee, A.; Andrew, H.; Patricia, A.; Samuelkamaleshkumar, S.; Prakash, H.; Sujatha, S.; Balasubramanian, S.; et al. Plug-and-train robot (pluto) for hand rehabilitation: Design and preliminary evaluation. *IEEE Access* **2021**, *9*, 134957–134971.
3. Nehrujee, A.; Prabhakar, A.; Balaraman, S.; Bombatkar, R.; Prakash, H.; Samuelkamaleshkumar, S.; Aaron, S.; Bhattacharji, S.; Sujatha, S.; Balasubramanian, S. The facilitators and barriers to home-based robotic rehabilitation in India: a pilot feasibility study. *Frontiers in Stroke* **2024**, *2*, 1265702.
4. Aguirre-Ollinger, G.; Chua, K.S.G.; Ong, P.L.; Kuah, C.W.K.; Plunkett, T.K.; Ng, C.Y.; Khin, L.W.; Goh, K.H.; Chong, W.B.; Low, J.A.M.; et al. Telerehabilitation using a 2-D planar arm rehabilitation robot for hemiparetic stroke: a feasibility study of clinic-to-home exergaming therapy. *Journal of NeuroEngineering and Rehabilitation* **2024**, *21*, 207.
5. Rätz, R.; Conti, F.; Müri, R.M.; Marchal-Crespo, L. A novel clinical-driven design for robotic hand rehabilitation: combining sensory training, effortless setup, and large range of motion in a palmar device. *Frontiers in neurorobotics* **2021**, *15*, 748196.
6. Devittori, G.; Ranzani, R.; Song, J.; Dinacci, D.; Petrillo, C.; Rossi, P.; Gassert, R.; Lambercy, O. Design Considerations and Pilot Usability Evaluation of ReHandyBot, A Portable Device for Upper Limb Therapy

- Along the Continuum of Care. In Proceedings of the International Conference on NeuroRehabilitation. Springer, 2024, pp. 263–267.
7. Lo, A.C.; Guarino, P.D.; Richards, L.G.; Haselkorn, J.K.; Wittenberg, G.F.; Federman, D.G.; Ringer, R.J.; Wagner, T.H.; Krebs, H.I.; Volpe, B.T.; et al. Robot-assisted therapy for long-term upper-limb impairment after stroke. *New England Journal of Medicine* **2010**, *362*, 1772–1783.
 8. De Iaco, L.; Veerbeek, J.M.; Ket, J.C.; Kwakkel, G. *Neurology* **2024**, *103*.
 9. Kaplan, S.H.; Billimek, J.; Sorkin, D.H.; Ngo-Metzger, Q.; Greenfield, S. Who can respond to treatment?: identifying patient characteristics related to heterogeneity of treatment effects. *Medical Care* **2010**, *48*, S9–S16.
 10. Norbury, A.; Seymour, B. Response heterogeneity: Challenges for personalised medicine and big data approaches in psychiatry and chronic pain. *F1000Research* **2018**, *7*, 55.
 11. Rymer, W.Z.; Reinkensmeyer, D. Precision Rehabilitation: Can Neurorehabilitation Technology Help Make It a Realistic Target? In *Neurorehabilitation Technology*; Springer, 2022; pp. 357–365.
 12. Cotton, R.J.; Seamon, B.A.; Segal, R.L.; Davis, R.D.; Sahu, A.; McLeod, M.M.; Celnik, P.; Ramey, S.L. A Causal Framework for Precision Rehabilitation **2024**. [[2411.03919](https://doi.org/10.1186/s12984-016-0148-3)].
 13. Liew, S.L.; Cotton, R.J.; Burdet, E.; Bermúdez i Badia, S.; Celnik, P.; Cole, J.H.; Liu, R.; Soekadar, S.R.; Winstein, C.; Schweighofer, N. Collaborative AI for precision neurorehabilitation: a roadmap. *Journal of NeuroEngineering and Rehabilitation* **2025**.
 14. Reinkensmeyer, D.J.; Burdet, E.; Casadio, M.; Krakauer, J.W.; Kwakkel, G.; Lang, C.E.; Swinnen, S.P.; Ward, N.S.; Schweighofer, N. Computational neurorehabilitation: modeling plasticity and learning to predict recovery. *Journal of NeuroEngineering and Rehabilitation* **2016**, *13*, 42. <https://doi.org/10.1186/s12984-016-0148-3>.
 15. Rowe, J.B.; Chan, V.; Ingemanson, M.L.; Cramer, S.C.; Wolbrecht, E.T.; Reinkensmeyer, D.J. Robotic assistance for training finger movement using a hebbian model: a randomized controlled trial. *Neurorehabilitation and neural repair* **2017**, *31*, 769–780.
 16. Ingemanson, M.L.; Rowe, J.R.; Chan, V.; Wolbrecht, E.T.; Reinkensmeyer, D.J.; Cramer, S.C. Somatosensory system integrity explains differences in treatment response after stroke. *Neurology* **2019**, *92*, e1098–e1108.
 17. Riley, J.D.; Le, V.; Der-Yeghiaian, L.; See, J.; Newton, J.M.; Ward, N.S.; Cramer, S.C. Anatomy of stroke injury predicts gains from therapy. *Stroke* **2011**, *42*, 421–426.
 18. Pila, O.; Duret, C.; Koepfel, T.; Jamin, P. Performance-based robotic training in individuals with subacute stroke: differences between responders and non-responders. *Sensors* **2023**, *23*, 4304.
 19. Farrens, A.J.; Garcia-Fernandez, L.; Rojas, R.D.; Estrada, J.O.; Reinsdorf, D.; Chan, V.; Gupta, D.; Perry, J.; Wolbrecht, E.; Do, A.; et al. Tailored robotic training improves hand function and proprioceptive processing in stroke survivors with proprioceptive deficits: A randomized controlled trial. *arXiv preprint arXiv:2511.00259* **2025**.
 20. Smith, M.C.; Ackerley, S.J.; Barber, P.A.; Byblow, W.D.; Stinear, C.M. PREP2 algorithm predictions are correct at 2 years poststroke for most patients. *Neurorehabilitation and neural repair* **2019**, *33*, 635–642.
 21. Millot, S.; Daghens, L.; Checkouri, T.; Wittwer, A.; Valabregue, R.; Galanaud, D.; Lamy, J.C.; Rosso, C. Prediction of upper limb motor recovery by the PREP2 algorithm in a nonselected population: external validation and influence of cognitive syndromes. *Neurorehabilitation and Neural Repair* **2024**, *38*, 764–774.
 22. Hayward, K.S.; Schmidt, J.; Lohse, K.R.; Peters, S.; Bernhardt, J.; Lannin, N.A.; Boyd, L.A. Are we armed with the right data? Pooled individual data review of biomarkers in people with severe upper limb impairment after stroke. *NeuroImage: Clinical* **2017**, *13*, 310–319.
 23. Whyte, J. A grand unified theory of rehabilitation (we wish!). The 57th John Stanley Coulter Memorial Lecture. *Archives of physical medicine and rehabilitation* **2008**, *89*, 203–209.
 24. Hart, T.; Dijkers, M.P.; Whyte, J.; Turkstra, L.S.; Zanca, J.M.; Packel, A.; Van Stan, J.H.; Ferraro, M.; Chen, C. A theory-driven system for the specification of rehabilitation treatments. *Archives of Physical Medicine and Rehabilitation* **2019**, *100*, 172–180.
 25. Cunningham, S. *Causal inference: The mixtape*; Yale university press, 2021.
 26. Angrist, J.D.; Pischke, J.S. *Mastering' metrics: The path from cause to effect*; Princeton university press, 2014.
 27. Imbens, G.W.; Rubin, D.B. *Causal inference in statistics, social, and biomedical sciences*; Cambridge university press, 2015.
 28. David, A.; Subash, T.; Varadhan, S.K.M.; Melendez-Calderon, A.; Balasubramanian, S. A Framework for Sensor-Based Assessment of Upper-Limb Functioning in Hemiparesis. *Frontiers in Human Neuroscience* **2021**, *15*. <https://doi.org/10.3389/fnhum.2021.667509>.
 29. Kirk, D.E. *Optimal control theory: an introduction*; Courier Corporation, 2004.

30. Morehead, J.R.; Orban de Xivry, J.J. A synthesis of the many errors and learning processes of visuomotor adaptation. *BioRxiv* **2021**, pp. 2021–03.
31. Diedrichsen, J.; White, O.; Newman, D.; Lally, N. Use-Dependent and Error-Based Learning of Motor Behaviors. *Journal of Neuroscience* **2010**, *30*, 5159–5166. <https://doi.org/10.1523/JNEUROSCI.5406-09.2010>.
32. Spampinato, D.; Celnik, P. Multiple Motor Learning Processes in Humans: Defining Their Neurophysiological Bases. *The Neuroscientist* **2021**, *27*, 246–267. <https://doi.org/10.1177/1073858420939552>.
33. Therrien, A.S.; Wong, A.L. Mechanisms of human motor learning do not function independently. *Frontiers in Human Neuroscience* **2022**, *15*, 785992.
34. Haith, A.M.; Krakauer, J.W. Model-based and model-free mechanisms of human motor learning. In *Progress in motor control: Neural, computational and dynamic approaches*; Springer, 2013; pp. 1–21.
35. Heald, J.B.; Lengyel, M.; Wolpert, D.M. Contextual inference underlies the learning of sensorimotor repertoires. *Nature* **2021**, *600*, 489–493.
36. Schölkopf, B. Causality for machine learning. In *Probabilistic and causal inference: The works of Judea Pearl*; 2022; pp. 765–804.
37. Leviton, L.C.; Lipsey, M.W. A big chapter about small theories: Theory as method: Small theories of treatments. *New Directions for Evaluation* **2007**, *2007*, 27–62.
38. Pearl, J. *Causality*; Cambridge university press, 2009.
39. Krebs, H.I.; Hogan, N.; Aisen, M.L.; Volpe, B.T. Robot-aided neurorehabilitation. *IEEE transactions on rehabilitation engineering* **1998**, *6*, 75–87.
40. Klein, J.; Spencer, S.; Allington, J.; Bobrow, J.E.; Reinkensmeyer, D.J. Optimization of a parallel shoulder mechanism to achieve a high-force, low-mass, robotic-arm exoskeleton. *IEEE Transactions on Robotics* **2010**, *26*, 710–715.
41. Klein, J.; Spencer, S.J.; Reinkensmeyer, D.J. Breaking it down is better: haptic decomposition of complex movements aids in robot-assisted motor learning. *IEEE Transactions on Neural Systems and Rehabilitation Engineering* **2012**, *20*, 268–275.
42. Milot, M.H.; Spencer, S.J.; Chan, V.; Allington, J.P.; Klein, J.; Chou, C.; Bobrow, J.E.; Cramer, S.C.; Reinkensmeyer, D.J. A crossover pilot study evaluating the functional outcomes of two different types of robotic movement training in chronic stroke survivors using the arm exoskeleton BONES. *Journal of neuroengineering and rehabilitation* **2013**, *10*, 112.
43. Guadagnoli, M.A.; Lee, T.D. Challenge point: a framework for conceptualizing the effects of various practice conditions in motor learning. *Journal of motor behavior* **2004**, *36*, 212–224.
44. Arsalan, M.; Ashish, G.; Yashendra, S. The role of augmented feedback on motor learning: A systematic review. *Cureus* **2021**, *13*.
45. Schmidt, R.A.; Lee, T.D.; Winstein, C.; Wulf, G.; Zelaznik, H.N. *Motor control and learning: A behavioral emphasis*; Human kinetics, 2018.
46. Wulf, G.; Shea, C.; Lewthwaite, R. Motor skill learning and performance: a review of influential factors. *Medical education* **2010**, *44*, 75–84.
47. Cordo, P.; Wolf, S.; Rymer, W.Z.; Byl, N.; Stanek, K.; Hayes, J.R. Assisted movement with proprioceptive stimulation augments recovery from moderate-to-severe upper limb impairment during subacute stroke period: a randomized clinical trial. *Neurorehabilitation and Neural Repair* **2022**, *36*, 239–250.
48. Carson, R.G.; Buick, A.R. Neuromuscular electrical stimulation-promoted plasticity of the human brain. *The Journal of physiology* **2021**, *599*, 2375–2399.
49. Sigrist, R.; Rauter, G.; Riener, R.; Wolf, P. Augmented visual, auditory, haptic, and multimodal feedback in motor learning: a review. *Psychonomic bulletin & review* **2013**, *20*, 21–53.
50. Stokic, D.S.; Dobbs, K.B.; Novotny, O.N. The OPTIMAL theory trifecta: bridging the gap to rehabilitation practice, 2025.
51. Marchal-Crespo, L.; Reinkensmeyer, D.J. Review of control strategies for robotic movement training after neurologic injury. *Journal of neuroengineering and rehabilitation* **2009**, *6*, 20.
52. Piovesan, D. A computational index to describe slacking during robot therapy. In *Progress in Motor Control: Theories and Translations*; Springer, 2016; pp. 351–365.
53. Goikoetxea-Sotelo, G.; van Hedel, H.J. Defining, quantifying, and reporting intensity, dose, and dosage of neurorehabilitative interventions focusing on motor outcomes. *Frontiers in Rehabilitation Sciences* **2023**, *4*, 1139251.

54. Hayward, K.S.; Churilov, L.; Dalton, E.J.; Brodtmann, A.; Campbell, B.C.; Copland, D.; Dancause, N.; Godecke, E.; Hoffmann, T.C.; Lannin, N.A.; et al. Advancing stroke recovery through improved articulation of nonpharmacological intervention dose. *Stroke* **2021**, *52*, 761–769.
55. World Health Organization. Towards a Common Language for Functioning, Disability and Health: ICF – The International Classification of Functioning, Disability and Health. ICF Beginner’s Guide, 2002. Accessed: 2026-01-28.
56. Gladstone, D.J.; Danells, C.J.; Black, S.E. The Fugl-Meyer assessment of motor recovery after stroke: a critical review of its measurement properties. *Neurorehabilitation and neural repair* **2002**, *16*, 232–240.
57. Saes, M.; Mohamed Refai, M.; van Beijnum, B.J.F.; Bussmann, J.; Jansma, E.P.; Veltink, P.H.; Buurke, J.H.; van Wegen, E.E.; Meskers, C.G.; Krakauer, J.; et al. Quantifying quality of reaching movements longitudinally post-stroke: a systematic review. *Neurorehabilitation and neural repair* **2022**, *36*, 183–207.
58. Balasubramanian, S.; Colombo, R.; Sterpi, I.; Sanguineti, V.; Burdet, E. Robotic assessment of upper limb motor function after stroke. *American journal of physical medicine & rehabilitation* **2012**, *91*, S255–S269.
59. Lydia, N.R.; Dukelow, S.P.; Scott, S.H. Impairments of the arm and hand are highly correlated during subacute stroke. *Journal of Rehabilitation Medicine* **2023**, *55*, 2174.
60. Connell, L.A.; Tyson, S. Measures of sensation in neurological conditions: a systematic review. *Clinical rehabilitation* **2012**, *26*, 68–80.
61. Dukelow, S.P.; Herter, T.M.; Moore, K.D.; Demers, M.J.; Glasgow, J.I.; Bagg, S.D.; Norman, K.E.; Scott, S.H. Quantitative assessment of limb position sense following stroke. *Neurorehabilitation and neural repair* **2010**, *24*, 178–187.
62. Lamercy, O.; Kim, Y.; Gassert, R. Robot-assisted assessment of vibration perception and localization on the hand. *Disability and Rehabilitation: Assistive Technology* **2013**, *8*, 129–135.
63. Zbytnewska, M.; Kanzler, C.M.; Jordan, L.; Salzman, C.; Liepert, J.; Lamercy, O.; Gassert, R. Reliable and valid robot-assisted assessments of hand proprioceptive, motor and sensorimotor impairments after stroke. *Journal of NeuroEngineering and Rehabilitation* **2021**, *18*, 115.
64. Winstein, C.; Lewthwaite, R.; Blanton, S.R.; Wolf, L.B.; Wishart, L. Infusing motor learning research into neurorehabilitation practice: a historical perspective with case exemplar from the accelerated skill acquisition program. *Journal of Neurologic Physical Therapy* **2014**, *38*, 190–200.
65. Hodges, N.J.; Lohse, K.R. An extended challenge-based framework for practice design in sports coaching. *Journal of Sports Sciences* **2022**, *40*, 754–768.
66. Gomes, E.; Alder, G.; Bright, F.A.; Signal, N. Understanding task “challenge” in stroke rehabilitation: an interdisciplinary concept analysis. *Disability and Rehabilitation* **2025**, *47*, 560–570.
67. Akizuki, K.; Ohashi, Y. Measurement of functional task difficulty during motor learning: What level of difficulty corresponds to the optimal challenge point? *Human movement science* **2015**, *43*, 107–117.
68. Akizuki, K.; Ohashi, Y. Salivary α -amylase reflects change in attentional demands during postural control: Comparison with probe reaction time. *Research Quarterly for Exercise and Sport* **2014**, *85*, 502–508.
69. Ma, Q.; Pei, G.; Meng, L. Inverted u-shaped curvilinear relationship between challenge and one’s intrinsic motivation: Evidence from event-related potentials. *Frontiers in Neuroscience* **2017**, *11*, 131.
70. Wulf, G.; Lewthwaite, R. Optimizing performance through intrinsic motivation and attention for learning: The OPTIMAL theory of motor learning. *Psychonomic bulletin & review* **2016**, *23*, 1382–1414.
71. Beroukhim-Kay, D.; Kim, B.; Monterosso, J.; Lewthwaite, R.; Winstein, C. Different patterns of neural activity characterize motor skill performance during acquisition and retention. *Frontiers in Human Neuroscience* **2022**, *16*, 900405.
72. Maclean, N.; Pound, P.; Wolfe, C.; Rudd, A. The concept of patient motivation: a qualitative analysis of stroke professionals’ attitudes. *Stroke* **2002**, *33*, 444–448.
73. Verrienti, G.; Raccagni, C.; Lombardozi, G.; De Bartolo, D.; Iosa, M. Motivation as a measurable outcome in stroke rehabilitation: a systematic review of the literature. *International journal of environmental research and public health* **2023**, *20*, 4187.
74. Meyns, P.; Roman de Mettelinge, T.; van der Spank, J.; Coussens, M.; Van Waelvelde, H. Motivation in pediatric motor rehabilitation: A systematic search of the literature using the self-determination theory as a conceptual framework. *Developmental neurorehabilitation* **2018**, *21*, 371–390.
75. Fan, X.; Xia, Y.; Wu, J.; Jia, S.; Hu, J. Influencing factors related to stroke patients’ rehabilitation motivation: a scoping review. *Frontiers in neurology* **2025**, *16*, 1615905.
76. Ryan, R.M.; Deci, E.L. Intrinsic and extrinsic motivations: Classic definitions and new directions. *Contemporary educational psychology* **2000**, *25*, 54–67.

77. Meng, L.; Pei, G.; Zheng, J.; Ma, Q. Close games versus blowouts: Optimal challenge reinforces one's intrinsic motivation to win. *International Journal of Psychophysiology* **2016**, *110*, 102–108.
78. van der Kooij, K.; in 't Veld, L.; Hennink, T. Motivation as a function of success frequency. *Motivation and Emotion* **2021**, *45*, 759–768.
79. Farrens, A.J.; Reinsdorf, D.; Garcia-Fernandez, L.; Rojas, R.D.; Chan, V.; Perry, J.; Wollbrecht, E.T.; Reinkensmeyer, D.J. Variants of active assist robotic therapy: feasibility of virtual assistance and proprioceptive training as gauged by their effects on success and motivation during finger movement training after stroke. *Journal of NeuroEngineering and Rehabilitation* **2025**, *22*, 167.
80. Chiviawosky, S. The motivational role of feedback in motor learning: Evidence, interpretations, and implications. In *Advancements in mental skills training*; Routledge, 2020; pp. 44–56.
81. Martinez, V.M.L.; Cardozo, P.; Kaefer, A.; Wulf, G.; Chiviawosky, S. Positive feedback enhances motivation and skill learning in adolescents. *Learning and Motivation* **2024**, *86*, 101966.
82. Oyake, K.; Yamauchi, K.; Inoue, S.; Sue, K.; Ota, H.; Ikuta, J.; Ema, T.; Ochiai, T.; Hasui, M.; Hirata, Y.; et al. A multicenter explanatory survey of patients' and clinicians' perceptions of motivational factors in rehabilitation. *Communications Medicine* **2023**, *3*, 78.
83. Yoshida, T.; Otaka, Y.; Kitamura, S.; Ushizawa, K.; Kumagai, M.; Yaeda, J.; Osu, R. Influence of motivation on rehabilitation outcomes after subacute stroke in convalescent rehabilitation wards. *Frontiers in neurology* **2023**, *14*, 1185813.
84. Winstein, C.J.; Wolf, S.L. Task-oriented training to promote upper extremity recovery. *Stein J, Harvey RL, Macko RF, Winstein CJ, Zorowitz Rd. Stroke Recovery and Rehabilitation. New York: Demos Medical* **2008**, pp. 267–290.
85. Ballester, B.R.; Ward, N.S.; Brander, F.; Maier, M.; Kelly, K.; Verschure, P.F. Relationship between intensity and recovery in post-stroke rehabilitation: a retrospective analysis. *Journal of Neurology, Neurosurgery & Psychiatry* **2022**, *93*, 226–228.
86. Teixeira, P.J.; Carraça, E.V.; Markland, D.; Silva, M.N.; Ryan, R.M. Exercise, physical activity, and self-determination theory: a systematic review. *International journal of behavioral nutrition and physical activity* **2012**, *9*, 78.
87. Naismith, H.; Dhillon, H.M.; Hunter, J.; Bultijnck, R.; Kneebone, A.; Hruby, G.; Eade, T.; Parker, L.; Campbell, R.; Yee, J. "I've got plenty of energy when I'm doing something I want to do": applying self-determination theory to exercise motivation in people with prostate cancer. *Supportive Care in Cancer* **2025**, *33*, 347.
88. Xu, Z.; Shamsulariffin, S.; Azhar, Y.; Xi, M. Does Self-Determination Theory Associate With Physical Activity? A Systematic Review of Systematic Review. *International Journal of Psychology* **2025**, *60*, e70044.
89. Salvalaggio, S.; Gambazza, S.; Andò, M.; Parrotta, I.; Burgio, F.; Danesin, L.; Busan, P.; Zago, S.; Mantini, D.; D'Imperio, D.; et al. Modeling upper limb rehabilitation-induced recovery after stroke: the role of attention as a clinical confounder. *Physical Therapy* **2025**, *105*, pzae148.
90. Thura, D.; Haith, A.M.; Derosiere, G.; Duque, J. The integrated control of decision and movement vigor. *Trends in Cognitive Sciences* **2025**.
91. Shadmehr, R.; Ahmed, A.A. Précis of vigor: neuroeconomics of movement control. *Behavioral and Brain Sciences* **2021**, *44*, e123.
92. Harris, C.M.; Wolpert, D.M. Signal-dependent noise determines motor planning. *Nature* **1998**, *394*, 780–784.
93. Novak, D.; Zihler, J.; Olenšek, A.; Milavec, M.; Podobnik, J.; Mihelj, M.; Munih, M. Psychophysiological responses to robotic rehabilitation tasks in stroke. *IEEE Transactions on neural systems and rehabilitation engineering* **2010**, *18*, 351–361.
94. Kumar, A.; Fang, Q.; Pirogova, E. The influence of psychological and cognitive states on error-related negativity evoked during post-stroke rehabilitation movements. *BioMedical Engineering Online* **2021**, *20*, 13.
95. Edwards, L.L.; King, E.M.; Bueteifisch, C.M.; Borich, M.R. Putting the "sensory" into sensorimotor control: the role of sensorimotor integration in goal-directed hand movements after stroke. *Frontiers in integrative neuroscience* **2019**, *13*, 16.
96. Bolognini, N.; Russo, C.; Edwards, D.J. The sensory side of post-stroke motor rehabilitation. *Restorative neurology and neuroscience* **2016**, *34*, 571–586.
97. Wang, H.; Wu, X.; Li, Y.; Yu, S. Efficacy of robot-assisted training on upper limb motor function after stroke: a systematic review and network meta-analysis. *Archives of Rehabilitation Research and Clinical Translation* **2025**, *7*, 100387.

98. Li, Y.; Lian, Y.; Chen, X.; Zhang, H.; Xu, G.; Duan, H.; Xie, X.; Li, Z. Effect of task-oriented training assisted by force feedback hand rehabilitation robot on finger grasping function in stroke patients with hemiplegia: a randomised controlled trial. *Journal of NeuroEngineering and Rehabilitation* **2024**, *21*, 77.
99. Mazzoleni, S.; Sale, P.; Tiboni, M.; Franceschini, M.; Carrozza, M.C.; Posteraro, F. Upper limb robot-assisted therapy in chronic and subacute stroke patients: a kinematic analysis. *American Journal of Physical Medicine & Rehabilitation* **2013**, *92*, e26–e37.
100. Goffredo, M.; Mazzoleni, S.; Gison, A.; Infarinato, F.; Pournajaf, S.; Galafate, D.; Agosti, M.; Posteraro, F.; Franceschini, M. Kinematic Parameters for Tracking Patient Progress during Upper Limb Robot-Assisted Rehabilitation: An Observational Study on Subacute Stroke Subjects. *Applied Bionics and Biomechanics* **2019**, *2019*, 4251089.
101. Balasubramanian, S.; Klein, J.; Burdet, E. Robot-assisted rehabilitation of hand function. *Current opinion in neurology* **2010**, *23*, 661–670.
102. Leech, K.A.; Roemmich, R.T.; Gordon, J.; Reisman, D.S.; Cherry-Allen, K.M. Updates in motor learning: implications for physical therapist practice and education. *Physical therapy* **2022**, *102*, p250.
103. Salazar, A.P.; Pinto, C.; Mossi, J.V.R.; Figueiro, B.; Lukrafka, J.L.; Pagnussat, A.S. Effectiveness of static stretching positioning on post-stroke upper-limb spasticity and mobility: Systematic review with meta-analysis. *Annals of physical and rehabilitation medicine* **2019**, *62*, 274–282.
104. Quattrocchi, G.; Greenwood, R.; Rothwell, J.C.; Galea, J.M.; Bestmann, S. Reward and punishment enhance motor adaptation in stroke. *Journal of Neurology, Neurosurgery & Psychiatry* **2017**, *88*, 730–736.
105. Galea, J.M.; Mallia, E.; Rothwell, J.; Diedrichsen, J. The dissociable effects of punishment and reward on motor learning. *Nature neuroscience* **2015**, *18*, 597–602.
106. Wolbrecht, E.T.; Chan, V.; Reinkensmeyer, D.J.; Bobrow, J.E. Optimizing compliant, model-based robotic assistance to promote neurorehabilitation. *IEEE Transactions on Neural Systems and Rehabilitation Engineering* **2008**, *16*, 286–297.
107. Casadio, M.; Sanguineti, V. Learning, retention, and slacking: a model of the dynamics of recovery in robot therapy. *IEEE Transactions on Neural Systems and Rehabilitation Engineering* **2012**, *20*, 286–296.
108. Blank, A.A.; French, J.A.; Pehlivan, A.U.; O'Malley, M.K. Current trends in robot-assisted upper-limb stroke rehabilitation: promoting patient engagement in therapy. *Current physical medicine and rehabilitation reports* **2014**, *2*, 184–195.
109. Subramanian, S.K.; Massie, C.L.; Malcolm, M.P.; Levin, M.F. Does provision of extrinsic feedback result in improved motor learning in the upper limb poststroke? A systematic review of the evidence. *Neurorehabilitation and neural repair* **2010**, *24*, 113–124.
110. Bai, Z.; Fong, K.N.; Zhang, J.J.; Chan, J.; Ting, K. Immediate and long-term effects of BCI-based rehabilitation of the upper extremity after stroke: a systematic review and meta-analysis. *Journal of neuroengineering and rehabilitation* **2020**, *17*, 57.
111. Chen, H.; Yun, G. Efficacy of Brain-Computer Interface Therapy for Upper Limb Rehabilitation in Chronic Stroke: Systematic Review and Meta-Analysis of Randomized Controlled Trials. *Journal of Medical Internet Research* **2026**, *28*, e79132.
112. Hsieh, Y.w.; Wu, C.y.; Lin, K.c.; Yao, G.; Wu, K.y.; Chang, Y.j. Dose–response relationship of robot-assisted stroke motor rehabilitation: the impact of initial motor status. *Stroke* **2012**, *43*, 2729–2734.
113. Duret, C.; Pila, O.; Grosmaire, A.G.; Koepfel, T. Can robot-based measurements improve prediction of motor performance after robot-assisted upper-limb rehabilitation in patients with moderate-to-severe sub-acute stroke? *Restorative Neurology and Neuroscience* **2019**, *37*, 119–129.
114. Kahn, L.E.; Zygmant, M.L.; Rymer, W.Z.; Reinkensmeyer, D.J. Robot-assisted reaching exercise promotes arm movement recovery in chronic hemiparetic stroke: a randomized controlled pilot study. *Journal of neuroengineering and rehabilitation* **2006**, *3*, 12.
115. Kahn, L.E.; Lum, P.S.; Rymer, W.Z.; Reinkensmeyer, D.J. Robot-assisted movement training for the stroke-impaired arm: Does it matter what the robot does? *The Journal of Rehabilitation Research and Development* **2006**, *43*, 619–630. <https://doi.org/10.1682/JRRD.2005.03.0056>.
116. Choudhuri, R.; Solomon, J.; Nehrujee, A.; Sujatha, S.; Balasubramanian, S. Effect of Role of Robotic Assistance on Upper-limb Sensorimotor Recovery: A Systematic Review and Meta-Analysis. *medRxiv* **2025**, pp. 2025–04.
117. Reinkensmeyer, D.J.; Housman, S.J. "If I can't do it once, why do it a hundred times?": Connecting volition to movement success in a virtual environment motivates people to exercise the arm after stroke. In Proceedings of the 2007 Virtual Rehabilitation. IEEE, 2007, pp. 44–48.

118. Ethier, C.; Gallego, J.; Miller, L.E. Brain-controlled neuromuscular stimulation to drive neural plasticity and functional recovery. *Current opinion in neurobiology* **2015**, *33*, 95–102.
119. Suvrathan, A. Beyond STDP—towards diverse and functionally relevant plasticity rules. *Current opinion in neurobiology* **2019**, *54*, 12–19.
120. Balasubramanian, S.; Melendez-Calderon, A.; Burdet, E. A robust and sensitive metric for quantifying movement smoothness. *IEEE transactions on biomedical engineering* **2011**, *59*, 2126–2136.
121. Balasubramanian, S.; Melendez-Calderon, A.; Roby-Brami, A.; Burdet, E. On the analysis of movement smoothness. *Journal of neuroengineering and rehabilitation* **2015**, *12*, 112.
122. Melendez-Calderon, A.; Shirota, C.; Balasubramanian, S. Estimating movement smoothness from inertial measurement units. *Frontiers in bioengineering and biotechnology* **2021**, *8*, 558771.
123. Ellis, M.D.; Sukal-Moulton, T.; Dewald, J.P. Progressive shoulder abduction loading is a crucial element of arm rehabilitation in chronic stroke. *Neurorehabilitation and neural repair* **2009**, *23*, 862–869.
124. Patton, J.L.; Mussa-Ivaldi, F.A. Robot-assisted adaptive training: custom force fields for teaching movement patterns. *IEEE Transactions on Biomedical Engineering* **2004**, *51*, 636–646.
125. Patton, J.L.; Huang, F.C. Error augmentation and the role of sensory feedback. In *Neurorehabilitation technology*; Springer, 2011; pp. 73–85.
126. Lum, P.S.; Burgar, C.G.; Shor, P.C. Evidence for improved muscle activation patterns after retraining of reaching movements with the MIME robotic system in subjects with post-stroke hemiparesis. *IEEE Transactions on Neural Systems and Rehabilitation Engineering* **2004**, *12*, 186–194.
127. Stein, J.; Krebs, H.I.; Frontera, W.R.; Fasoli, S.E.; Hughes, R.; Hogan, N. Comparison of two techniques of robot-aided upper limb exercise training after stroke. *American journal of physical medicine & rehabilitation* **2004**, *83*, 720–728.
128. Hardwick, R.M.; Rajan, V.A.; Bastian, A.J.; Krakauer, J.W.; Celnik, P.A. Motor learning in stroke: trained patients are not equal to untrained patients with less impairment. *Neurorehabilitation and neural repair* **2017**, *31*, 178–189.
129. Aglietti, V.; Lu, X.; Paleyes, A.; González, J. Causal bayesian optimization. In Proceedings of the International Conference on Artificial Intelligence and Statistics. PMLR, 2020, pp. 3155–3164.

Disclaimer/Publisher's Note: The statements, opinions and data contained in all publications are solely those of the individual author(s) and contributor(s) and not of MDPI and/or the editor(s). MDPI and/or the editor(s) disclaim responsibility for any injury to people or property resulting from any ideas, methods, instructions or products referred to in the content.